The Functions of Clusterin Expression in Renal Mesenchymal Stromal Cells: Regulation of Cell Proliferation and Macrophage Activation

xiaodong weng
Renmin Hospital of Wuhan University
Jing Li
Huazhong University of Science and Technology
Qiunong Guan
University of British Columbia
Haimei Zhao
Jiangxi University of Traditional Chinese Medicine
Zihuan Wang
Southern Medical University
Martin Gleave
University of British Columbia
Christopher Nguan
University of British Columbia
Caigan DU (caigan@mail.ubc.ca)
University of British Columbia

Research Article

Keywords: Clusterin, renal mesenchymal stem cells, proliferation, macrophage

Posted Date: September 1st, 2021

DOI: https://doi.org/10.21203/rs.3.rs-529324/v2

Abstract

The expression of clusterin (CLU) in mice increases resistance to renal ischemia-reperfusion injury and promotes renal tissue repair. However, the mechanisms underlying of the renal protection of CLU remain largely unknown. Mesenchymal stromal cells (MSCs), found in different compartments of the kidney, may contribute to kidney cell turnover and injury repair. This study investigated the in vitro functions of CLU in kidney mesenchymal stromal cells (KMSCs). KMSCs were isolated by digestion of kidney tissues with collagenase type 1 and growth in plastic culture plates. Cell surface markers, apoptosis and phagocytosis were determined by flow cytometry, and CLU protein by Western blot. Here, we showed that KMSCs isolated from both wild type (WT) and CLU knockout (KO) mice positively expressed CD133, Sca-1, CD44, and CD117, and negatively of CD34, CD45, CD163, CD41, CD276, CD138 and CD79a. There was no difference in trilineage differentiation to chondrocytes, adipocytes and osteocytes between WT and KO KMSCs. CLU protein was expressed in and secreted by WT KMSCs, and it was up-regulated in response to hypoxia. However, lack of CLU expression did not negatively affect hypoxia-induced apoptosis in cultured KMSCs. The WT KMSCs proliferated faster than KO KMSCs in cultures. Furthermore, the incubation of macrophages with CLU-containing culture medium from WT KMSCs increased the CD206 expression in the macrophages and their phagocytic capacity. In conclusion, our data for the first time demonstrate the functions of CLU in the promotion of KMSCs proliferation, and may be required for KMSCs-regulated macrophage M2 polarization and phagocytic activity.

Introduction

Mesenchymal stromal/stem cells (MSCs) are self-renewal, multipotent, fibroblast-like adult cells that have been found in a variety of adult tissues in our body[1]. Accumulating evidence in literature indicates that these cells play a significant role in self-repair and have therapeutic potential for many different diseases[1–3]. Indeed, multipotent kidney-derived MSCs (KMSCs) are found in the interstitial space of adult mouse kidneys[4] or in the perivascular space and the capsule of adult human kidneys[5, 6]. Similar to other types of MSCs, KMSCs have high capacity of immunomodulation such as inactivation of dendritic cells and T cells[4–8]. When injected into the renal parenchyma, these KMSCs can integrate into the interstitial compartment or the renal tubule of the kidney and accelerate tubular growth or repair after kidney injury[4, 6, 9]. The evidence from these studies may suggest the potential of KMSCs specifically for kidney repair and regeneration. However, the molecular mechanisms underlying the immunomodulation, tubular repair and differentiation of KMSCs are poorly understood.

Clusterin (CLU) is a 75–80 kDa multifunctional heterodimeric glycoprotein. This protein involves in numerous pathophysiological processes such as cancer progression, aging, dry eye disease, neurodegenerative disorders, metabolic/cardiovascular diseases and immune diseases[10, 11], in which CLU plays a role in the regulation of cell apoptosis, proliferation, tissue remodeling, lipid transport, complement inhibition, and carcinogenesis[12]. In addition, we and others have demonstrated that genetic knockout (KO) of CLU expression accelerates the progression of kidney disease, including the renal

fibrosis in response to unilateral ureteral obstruction (UUO) and ischemia-reperfusion injury (IRI),[13, 14] and progressive glomerulopathy in aging mice[15]. Particularly interestedly, CLU KO mice experience more severe renal IRI and the delay of renal repair after IRI as compared to wild type (WT) counterparts[16, 17]. However, the mechanisms by which a lack of CLU expression causes more kidney injury and/or delays its repair are not fully understood. The objective of this study was designed to investigate the impact of CLU deficiency in the activities of KMSCs in CLU KO mice as compared to WT mice in vitro experimental systems.

Methods And Materials

Animals

Both WT C57BL/6 (B6) and CLU KO mice in B6 background (B6-Clu$^{-/-}$) (total 10 mice per group) were received from the breeding colonies in the animal facility at the Jack Bell Research Centre (Vancouver, BC, Canada). All the animals (males, 8–12 weeks old, 20–30 g bodyweight) for the experiments were cared and used in accordance with the Canadian Council on Animal Care guideline under the protocols (A18-0035; A16-0271) approved by the Animal Use Subcommittee at the University of British Columbia (Vancouver, BC, Canada). This study was carried out in compliance with the ARRIVE guidelines (https://arriveguidelines.org) along with the Essential 10 in the guidelines present in this manuscript.

Isolation and culture of mouse KMSCs

The KMSCs were isolated from the kidney of WT or CLU KO mice as described by Ashwani Kumar Gupta[18]. In brief, the kidney tissues were minced and digested with 0.1% collagenase type I (Sigma-Aldrich Canada) in serum free DMEM medium (Gibco, NY, United States) for 30 min at 37 ℃ with intermittent stirring in water bath. After washing twice with the DMEM medium, the digested tissues were filtered by using a 40 µm Nylon mesh (Fisherbrand) cell strainer, followed by incubation with red blood cell lysis buffer [0.15 M NH_4Cl, 1.0 mM $KHCO_3$, 0.1 mM Ethylenediaminetetraacetic acid (EDTA), pH 6.8] for 5 min. After washing two more times, cells were cultured in plastic culture plates (BD, New Jersey, United States) in 15% fetal bovine serum (FBS)-containing DMEM medium (Gibco, NY, United States) at 37°C in a culture incubator with 5% CO_2. After 2 days of cell seeding, the culture media containing non-adherent cells were replaced with the fresh medium, and remaining adherent cells were continuously cultured in the plastic culture plates. The cells from cultures at passage 4 (P4) to 15 (P15) were used for the experiments.

Isolation of microvesicles

The monolayers (80% confluence) of KMSCs were grown in the DMEM medium containing 5% of pooled serum from CLU KO mice at 37°C in the culture incubator with 5% CO_2 for 4 days, followed by harvesting the conditioned medium. A two-step different centrifugation was used for the isolation of the microvesicles from the conditional medium. The first step was to pellet dead cells and large cell debris by

the centrifugations of the samples at 2,000 ×g for 20 min, and the resultant supernatants were collected and transferred to new tubes. Then the supernatants were ultracentrifuged at 20,000 ×g for 30 min at 4°C to pellet the microvesicles. The microvesicle pellets were washed with ice-cold PBS to remove proteins. The protein fraction in the supernatants from both centrifugation steps was precipitated by 80% saturated ammonium sulfate solution. All the pellets and protein fractions of the supernatants were collected for Western blot analysis of CLU protein.

Flow cytometric analysis of cell surface markers on KMSCs

The cell surface markers of KMSCs were determined by fluorescence activated cell sorting (FACS) analysis using a panel of fluorescent dye-conjugated antibodies (*e*Bioscience, San Diego, CA, USA): rat monoclonal anti-mouse CD133-phycoerythrin (PE) (13A4), rat monoclonal anti-mouse Sca-1-Alexa Fluor 700 (D7), rat monoclonal anti-mouse CD44-allophycocyanin (APC) (KM201), rat monoclonal anti-mouse CD117-Alexa Fluor 700 (ACK2), rat monoclonal anti-mouse CD34-fluorescein isothiocyanate (FITC) (RAM34), rat monoclonal anti-mouse CD45-PE (30-F11), rat monoclonal anti-mouse CD163-PE (TNKUPJ), rat monoclonal anti-mouse CD41-PE (MWReg30), rat monoclonal anti-mouse CD276-PE (M3.2D7), rat monoclonal anti-mouse CD138-PE (300506) and mouse monoclonal anti-CD79a-PE (HM47), following manufacture's protocol (*e*Bioscience). Briefly, KMSCs ($2.5 \cdot 10^5$) in PBS containing 1% of FBS were incubated with 1 μL of antibody solution for 30 min at room temperature. After washing with PBS, the positive cells were counted by using a FacsCanto II (BD Biosciences) and further quantified using FlowJo software (Tree Star Inc., Ashland, OR, USA).

Trilineage differentiation to chondrocytes, osteocytes or adipocytes

KMSCs were harvested from cultures after P5, and their potential for differentiation to chondrocytes, osteocytes or adipocytes was examined as previously described by Liu et al.[19]. The chondrogenic differentiation of KMSCs was confirmed by positive staining of cartilage formation in the cells with 1% of acidic Alcian blue in 80% methanol (v/v) (pH 2.5), the osteogenic differentiation was confirmed by positive staining of $Ca2^+$ matrix mineralization with 2% Alizarin red S in 0.5% NH_4OH (pH 4.2), and the adipogenic differentiation was examined by the presence of intracellular lipid droplets stained with Oil red O.

Hypoxia and Western blot assay

KMSCs were incubated in the O_2-Control-InVitro-Glove-Box (Coy Laboratory, Michigan, USA) under hypoxic condition (1% O_2, 5% CO_2 and 94% N_2) for different periods of time (day 0 to day3). The total cellular protein was extracted from the KMSCs at these time points, and CLU expression was examined by Western blot. Briefly, protein samples (50 μg/sample) were fractionated by 10% SDS-PAGE and then transferred onto nitrocellulose membrane. The CLU protein in the blot was identified with primary goat polyclonal anti-CLU antibody (Santa Cruz Biotechnology, Santa Cruz, CA) and secondary donkey anti-goat IgG H&L-Alexa Fluor® 680 (Abcam). The CLU protein-antibodies was viewed by using Odyssey (LI-COR,

Inc., Lincoln, Nebraska, USA). Blots were reprobed using β-actin (Sigma-Aldrich Canada) for confirmation of loaded protein in each sample.

Determination of apoptosis

Apoptosis of KMSCs under the hypoxia for three days was measured by FACS analysis with Annexin-V-PE for staining of early apoptosis and 7-Aminoactinomycin D (7-AAD for late apoptosis as described before[17]. Briefly, KMSCs were cultured under the hypoxia as mentioned above for three days, and were harvested by a brief incubation with trypsin-EDTA solution (Sigma-Aldrich). The apoptotic cells were stained with Annexin-V-PE and 7-ADD in 1×binding buffer for 15 min. The intensity of staining fluorescence was measured by a FACS and analyzed as compared with background controls using FlowJo software (Tree Star Inc.).

MTT assay

The MTT assay is a colorimetric method of specifically measuring the activity of NAD(P)H-dependent oxidoreductase as an indicator of a viable cell number. Briefly, KMSCs were seeded in 96-well plates at the density of 2×10^3 cells/well. After overnight incubation, MTT (10 μL, 5 mg/mL) was added and incubated for 2 h, cells were dissolved in 100 μL DMSO/well, and the optical density (OD) at 490 nm was measured with a microplate reader (BioTek, Winooski, VT, USA).

Flow cytometric analysis of macrophage phenotypes

The phenotypes of macrophage RAW264.7 cells were determined by the FACS analysis of cell surface expression of CD80, a M1 phenotype marker, or CD206, a M2 phenotype marker as described above. In brief, RAW264.7 cells (5×10^4 cells/well) in 10% FBS DMEM medium were seeded in 24-well plates for overnight, followed by incubation with a mixture of 50% of the supernatant of KMSCs cultures and 50% of fresh 10% FBS DMEM medium for 24 h. Then the cells were stained with rat monoclonal anti-mouse CD80-FITC (1G10) (*e*Bioscience) or rat monoclonal anti-mouse CD206-PE (MR6F3) (*e*Bioscience) in the dark for 30 min at 4°C. After washing with PBS twice, the positive stain of CD80 and CD206 on RAW264.7 cells was counted by using a FACS and further quantified using FlowJo software (Tree Star Inc.), respectively.

Phagocytosis Assay

The phagocytic activity of RAW264.7 cells was measured by using fluorescence-labeled latex beads (Sigma-Aldrich Canada, L-3030) as described previously[20]. In brief, RAW264.7 cells in 24-well plates were treated with the supernatant from KMSCs cultures for 24 h as described above, followed by incubation with 2.0 μL of fluorescent latex beads per well for 2 h. Phagocytosis was determined by the number of cells engulfing beads, which was measured by using the FACS and was presented as the increased intensity of fluorescence (%) in RAW264.7 cells as compared to background controls (no beads) using FlowJo software (Tree Star Inc.).

Statistical analysis

Data were collected from at least three separate experiments in each study, and were presented as mean ± standard deviation (SD) or standard error of the mean (SEM) for each group in the text. The difference between groups was analyzed using t-tests or analysis of variance (ANOVA) as appropriate with GraphPad Prism 7 (GraphPad Software, Inc., La Jolla, CA, USA). A p value of ≤ 0.05 was considered significant.

Results

CLU expression in KMSCs from WT mice

The expression of CLU, both intracellular and secreted CLU proteins, in cultured KMSCs was examined by Western blot. As shown in Fig. 1A and B, the KMSCs isolated from WT mice (WT KMSCs) expressed the intracellular CLU in the cellular protein extracts and secreted mature CLU (mCLU) in the culture supernatants, whereas these protein bands were absent in KMSCs from CLU KO mice. In addition, the intracellular CLU - CLU precursor (Pre-CLU) in WT KMSCs was upregulated in response to hypoxia (Fig. 1A).

To verify if mCLU presented in the microvesicles secreted from the KMSCs, the monolayer of KMSCs was grown in the DMEM medium containing 5% pooled serum from CLU KO mice in a 5% CO_2 incubator at 37℃ for 4 days, and the secreted microvesicles in the culture medium were isolated by centrifugation at 20,000 ×g. As shown in Fig. 1C, the presence of CLU protein was seen in cellular protein extracts, dead cells or cell debris and supernatants, but not in microvesicle fractions. The sizes and morphology of the isolated microvesicles from WT KMSCs were not different from those from KO MSCs (Fig. 1D). These data might suggest that mCLU was not associated with the secreted microvesicles but a soluble factor secreted from the KMSCs.

The effect of CLU expression on the morphology of KMSCs in plastic culture dishes

The minimal criteria for defining MSCs include physical adherence to plastic culture dishes, fibroblast-like morphology in culture, positive and negative expression of specific cell surface markers and multipotential for differentiation to chondrocytes, osteocytes or adipocytes[21, 22]. The morphology and adherent property of KMSCs from CLU KO mice as compared to WT mice in the plastic culture dishes was examined by using a microscope. As shown in Fig. 2, there was little difference of morphologic changes and physical adherence to the plastic culture dishes between WT and KO KMSCs in cultures from P1 to P15. In P1 cultures after 2 weeks of incubation, there were some cells in both groups that exhibited fibroblast-like spindle shape, and after P4 the number of cells with spindle-shaped fibroblast-like morphology was gradually increased, and these cells were propagated well in the plastic culture dishes and reached a significant level after the P5. These data suggested that the KMSCs from CLU KO mice were not different from WT mice in the morphology and adherent property.

The effect of CLU expression on the expression of cell surface markers of KMSCs

The MSC-specific cell surface markers of KMSCs at P4 from both WT and CLU KO mice were examined by using FACS analysis. As shown in Fig. 3, the KMSCs from both groups were strong positive in the expression of CD133, Sca-1, CD44, and CD117, and negative in CD45, CD163, CD41, CD276, CD138, CD79a (Fig. 3; Table 1). As compared to the background staining, there was a small proportion (5% -10% percentage) of the cells from both WT and KO KMSCs expressing CD34, suggesting that a small population of KMSC might weakly express this hematopoietic stem cell marker or the cells from hematopoietic system. These data suggested that the KMSCs from CLU KO mice were not different from WT mice in the expression of MSC-specific cell surface markers.

The effect of CLU on the multipotential of KMSCs for trilineage differentiation

The multipotential of KMSCs from CLU KO mice as compared to WT mice for their differentiation to chondrocytes, osteocytes or adipocytes was examined by using standard methods as described previously[19]. As shown in Fig. 4, the differentiation of KMSCs of both groups to adipocytes was seen after incubation with adipocygenic differentiation medium for 4 weeks, in which the lipid droplets in differentiated cells (adipocytes) were confirmed by oil red O-staining (right column). For osteogenic differentiation, a confluent monolayer with some “clustering” of osteocytes was observed after incubation with osteogenic differentiation medium for 4 weeks, indicated by alizarin red S staining of the extracellular calcium deposits (middle column). Similarly, the KMSCs from WT and CLU KO mice were differentiated to the phenotype of chondrocytes, indicated by the presence of Alcian blue-stained cartilage matrix (right column). Further, the chondrocytes in WT group were clustering but not in KO group. These data indicated that KMSCs from CLU KO mice had equal capability as WT groups of differentiating to the chondrocytes, osteocytes or adipocytes.

The effect of CLU on KMSCs survival in response to hypoxia

Hypoxic injury is an initial insult of IRI, and expression of CLU increases the survival of kidney tubular epithelial cells in hypoxia[17, 23] Here, the impact of CLU expression on KMSCs survival in hypoxia was investigated. The KMSCs from WT and CLU KO mice were incubated in hypoxia for three days, and cell survival or death was examined by both microscopy and FACS analyses. Microscopic examination revealed that there were barely dead cells in the KMSCs cultures of both group (Figs. 5b, 5d). Further FACS analysis confirmed the microscopic observation, indicated only (9.179 ± 0.6757, n = 8) and KO (10.02 ± 1.102, n = 8), which were not significantly different (Fig. 5e). These data suggest that a lack of CLU expression did not affect the survival of KMSCs in the hypoxic environment.

The effect of CLU on KMSCs proliferation in vitro

The difference of the cellular proliferation between WT and KO KMSCs was examined using MTT assay. As shown in Fig. 6, as compared to WT group, the growth rates of KO group were significantly slower (WT vs. KO: p = 0.0174, two-way ANOVA), especially at day 4 (p = 0.0189, two-way ANOVA multiple comparisons), day 5 (p = 0.0118, two-way ANOVA multiple comparisons), and day 6 (< 0.0001, two-way ANOVA multiple comparisons). Taken together, these data imply that the lack of CLU expression significantly reduced the proliferation of KMSCs.

The effect of KMSCs-secreted CLU on regulation of phenotypes and phagocytosis of macrophages

MSC-sourced secretome consists of MSC-derived bioactive factors (soluble proteins, nucleic acids, lipids and extracellular microvesicles) secreted to the extracellular space, and mediates the biological functions of MSCs [24, 25]. Here, the different effects of the secretome from KMSCs from CLU KO mice compared to WT mice on the phenotype of macrophage was examined by using FACS (Fig. 7). As shown in Fig. 7b, the supernatant or secretome from WT KMSCs more significantly upregulated the M2 marker CD206 expression than the secretome of KO KMSCs (WT: 52.875 ± 12.727, KO: 36.7 ± 14.696, p = 0.0392, n = 4, One-way ANOVA). As shown in Fig. 7c, the secrtome from either WT (37.972 ± 18.409) or KO KMSCs (30.425 ± 18.186) did not affect the M1 marker CD80 expression as compare to culture medium control (30.13 ± 19.387). Taken together, these data suggest that the WT KMSC-sourced secretome had more profound effect than those from KO KMSCs on the activation of M2 than M1.

The phagocytosis of macrophages affected by the supernatant or secretome from KO KMSCs as compared to that from WT KMSCs was examined by using FACS (Fig. 8). As shown in Fig. 8b, the supernatant or secretome from WT KMSC enhanced more phagocytosis of the macrophages than that from KO KMSCs, as indicated by 18.98 ± 3.379% in WT compared to 8.043 ± 1.052% in KO group (p = 0.005), and there was no significant difference between KO and normal control group (7.228 ± 0.314 %). Taken together, these data suggest that the supernatant or secretome from KMSCs of WT but not from CLU KO increased the phagocytosis function of macrophage.

Discussion

Multipotent kidney progenitor cells or KMSCs have been identified in different anatomical locations of adult kidneys of both humans and rodents [26, 27], including nontubular MSCs in renal interstitial space of mouse adult kidneys[4, 28] and progenitor-like cells in S3 segment of nephron in rat adult kidneys[29]. These KMSCs have been found to contribute to the regeneration or repair of renal endothelium and tubules after renal IRI[28, 30]. However, the molecular mechanisms by which KMSCs repair the kidney injury are not fully understood. We have previously demonstrated that as compared to CLU KO mice, CLU expression in mice is required for tissue repair and suppresses macrophages infiltration and proinflammatory M1 polarization in the kidney after IRI [16, 31]. In this study, we isolated KMSCs from the kidneys of both WT and CLU KO mice. There were not differences in the trilineage differentiation and

survival under hypoxic condition between WT and KO KMSCs. The WT KMSCs secreted CLU protein as a soluble factor that was not associated with secreted microvesicles. As compared to KO KMSCs, CLU-expressing KMSCs proliferated faster in culture, and the CLU-containing conditional medium from the KMSCs promoted anti-inflammatory M2 polarization and phagocytosis of macrophages.

MSCs are a heterogeneous population of fibroblast-like cells in culture and can be isolated from all different tissues in the body [32]. The essential standards for phenotypic and functional characterization of these cells have been initially recommended by the International Society for Cellular Therapy (ISCT); MSCs are plastic-adherent, have trilineage differentiation capacity (adipogenic, osteogenic, and chondrogenic) and express a cell surface profile of $CD73^+$, $CD90^+$, $CD105^+$, $CD11b^-$ /$CD14^-$, $CD19^-$/$CD79a^-$, $CD34^-$, $CD45^-$, and HLA-DR^-[22] In addition, the most common positive markers of CD29, CD44, CD90, and CD105 are recommended especially for adult MSCs in a recent systemic review[33] and the most prominent negative markers are CD34, CD45, and CD14 [33].. Similarly, the mouse kidney-derived MSCs or KMSCs have reported to be positive for CD29, CD44, Sca-1, CD73, CD105, and CD117 and negative for hematopoietic markers (e.g. CD11b, CD19, and CD45) [34–36]. In the present study, the plastic-adherent, spindle-shaped and fibroblast-like cells were isolated from the kidneys of both WT and CLU KO mice by culturing in plastic culture plates (Fig. 1). These cells from either WT or KO mice were highly expressed $CD133^+$ (Prom1), Sca-$1(Ly6a)^+$, $CD44^+$ and $CD117^+$(c-kit)(Fig. 2 and Table 1), which are also defined as prostate cancer stem cell phenotype[37]. In addition, these cells were almost negative in the expression of CD45, CD163, CD41, CD276, CD138 and CD79a, and the low expression of CD34, indicating that a small fraction of the isolated KMSCs were hematopoietic cells which represented “contamination” from intrarenal blood cells in our cultures. However, the “universal” stem cell markers such as CD133, CD24, Sca-1, and CD117 are also positively expressed in differentiated epithelia, including renal epithelia[38, 39]. CD133 was the most common marker for the phenotype of stem cells which provide protection in acute tubular and glomerular damage[40, 41], and it is also expressed in many different cell types, suggesting that a single marker is probably insufficient to identify a particular stem cell type[42]. In fact, one study has documented that both $CD133^+$ and $CD133^-$ cells improve renal function and promote renal regeneration to a similar degree[43]. The other studies indicate that the $CD133^+$/$CD24^+$ cells form both multicellular spheroids (nephrospheres) and branched tubule-like structures and undergo neurogenic, adipogenic, osteogenic differentiation, whereas the $CD133^-$/$CD24^+$ cells are unable to form these structures and unable to grow in some of the specialized differentiation media[44]. Indeed, there is no consensus among researchers regarding specific markers (alone or in combination) for identifying or isolating MSCs from the kidney.

In humans, there are two isoforms of CLU from the initial protein precursor, secretory CLU (sCLU, 75–80 kDa) and nuclear CLU (nCLU, 55 kDa), that differs in their functions[45, 46]. The sCLU is a major cytoprotective factor, while the nCLU is a cell death protein[45, 46]. However, only secretory CLU has been identified in mice[47]. Therefore, the biological functions of CLU in mice may only reflect those of sCLU in humans. Microvesicles secreted by MSCs are an important vehicle to transfer the proteins, mRNA and

miRNA from the MSCs to target cells, by which the target cell proliferation and differentiation are regulated[48]. In this study, we confirmed that CLU secreted by KMSCs was a soluble factor but not with the microvesicles (Fig. 1), suggesting that the functions of extracellular CLU outside the KMSCs are not mediated by the microvesicles. Further, a lack of CLU expression did not significantly affect the differentiation capacity of KMSCs to adipocytes, osteocytes, and chondrocytes in vitro (Fig. 4). However, recombinant sCLU protein treatment of mouse MSCs from the bone marrow inhibits the osteoblast differentiation while stimulates adipocyte differentiation[12]. The difference between our observations and this study may be due to the fact that the addition of recombinant sCLU and endogenous complete CLU gene knockout or only endogenous CLU may have different effects on trilineage differentiation. In this study, we also noticed that the lack of CLU expression obviously inhibited the “clustering” formation of the differentiated chondrocytes (Fig. 4). This finding is consistent with the ability of CLU to elicit clustering of Sertoli cells in an early study [49] and to suppress tubular epithelial cell migration[16, 50], suggesting that the differentiated chondrocytes secret CLU protein that is required for cluster formation via an autocrine manner, which however remains further investigation.

CLU expression is up-regulated in normal human diploid fibroblasts exposed to hypoxic conditions (1.5% O_2 or $CoCl_2$)[51]. Similar results have been seen in human kidney tubular epithelial cells (HKC-8) [23] and WT KMSCs (Fig. 1). The expression of CLU protein protects kidney epithelial cells from hypoxia-induced cells[23, 50]; however, it has no effect on KMSCs viability or death under prolonged hypoxia exposure (3 days) as no difference of cell death/viability between WT and KO KMSCs was seen (Fig. 5). The reasons why CLU cytoprotective activity against hypoxia is different between tubular epithelial cells and KMSCs remain unknown. It has been well known that hypoxia is a critical component for the maintenance of undifferentiated and slow-cycling proliferation states of a broader spectrum of stem cell niche[52, 53], and in the renal stem cell niche of papilla of adult kidneys, the oxygen tensions are less than 1% (4–10 mmHg) [54]. These findings simply imply that KMSCs may have unique anti-hypoxia feature for living in hypoxic microenvironment, as a result, the up-regulated CLU did not provide additional protection against hypoxia. These observations are supported by the fact that the renal progenitor cells have higher resistance to injury in comparison to all other differentiated cells of the kidney[52].

Recombinant sCLU protein stimulates the proliferation of mouse bone marrow-derived MSC[12]. Our previous studies demonstrated that the role of CLU in renal repair and tubular cell proliferation in culture is associated with up-regulation of a panel of genes that positively regulate cell cycle progression and DNA damage repair, which may promote cell proliferation but not involves epithelial cell migration[16, 50]. Here, the proliferation of KMSCs from WT and KO also been investigated and the results showed that CLU deficiency significantly inhibited the proliferation capacity of KMSCs (Fig. 6). Further, we observed the CLU gradually up-regulated in hypoxia (1% O^2) at day1 and day2 (Fig. 1), which is consistent with the faster proliferation of WT KMSCs under hypoxic conditions (Supplement data: Fig. 1). All of these data imply that CLU participates in the regulation of proliferation of KMSCs, which may contribute to kidney repair – more proliferating cells in WT than in CLU KO kidneys[16].

The renoprotective activity of MSCs is associated with their secreted cytokines, growth factors and other molecules that inhibit inflammation and fibrosis, and promote endogenous repair processes[42]. In the present study, the CLU-containing conditional medium from WT KMSCs significantly upregulated the M2 marker CD206 expression and not affected the M1 marker CD80 expression in macrophages (Fig. 7) and increased the phagocytosis of macrophages (Fig. 8). These results are consistent with our observations in vivo – the kidney repair in WT is associated with more infiltrating M2 macrophages[31] and are supported by that MSCs ameliorate acute kidney injury via the activation of macrophages to a trophic M2 phenotype[55]. It has been known that the M2 macrophages have higher phagocytosis capacity for clearance of apoptotic cells, produce extracellular matrix, mitigate inflammatory response, and promote wound healing [56, 57], suggesting that KMSCs is immunosuppressive mediators by upregulated the M2 polarization but not the M1 polarization through a paracrine action.

One has to acknowledge the limitations of this study. This study only focussed on the role of CLU in some characteristics (e.g. differentiation, survival, proliferation, and macrophage regulation) of KMSCs in culture. The biological functions of CLU in KMSCs in vivo were not investigated. We also did not investigate the molecular pathways by which CLU functions in KMSCs.

Conclusions

CLU KO results in more severe renal tissue damage and impairs renal repair after IRI[16, 17] and accelerates renal fibrosis in response to IRI and UUO[13, 14]. The present study indicates that CLU deficiency inhibits the proliferation of KMSCs and hinders the polarization-inducing ability of M2 macrophages and the ability to induce macrophage phagocytosis. Our data imply that CLU may play an important regulatory role in the involvement of KMSCs in various diseases and inflammatory injuries.

Abbreviations

CLU
clusterin
DMEM
Dulbecco’s modified Eagle’s medium
FACS
fluorescence activated cell sorting
FBS
Fetal bovine serum
HKC-8
human kidney tubular epithelial cells – 8
IRI
ischemia-reperfusion injury
ISCT

International Society for Cellular Therapy
KMSCs
kidney mesenchymal stromal cells
KO
knockout
MSCs
Mesenchymal stromal cells
MTT
3-(4,5-dimethylthiazol-2-yl)-2,5-diphenyltetrazolium bromide
nCLU
nuclear CLU
Pre-CLU
Clusterin precursor
sCLU
secretory CLU
SD
Standard deviation
SEM
Standard error of the mean
UUO
unilateral ureteral obstruction
WT
wild type

Declarations

Ethics approval and consent to participate

All the animals for the experiments were cared and used in accordance with the Canadian Council on Animal Care guideline under the protocol (A18-0035; A16-0271) approved by the Animal Use Subcommittee at the University of British Columbia (Vancouver, BC, Canada)

Consent for publication

Not applicable

Availability of data and materials

The datasets used and/or analysed to support the findings of this study are included within the article and are also available from the corresponding author (Caigan Du) upon request.

Competing interests

The authors declare that they have no competing interests.

Funding

This work was supported by the Canadian Institutes of Health Research (to CD) and by the China Scholarship Council (XW).

Authors' contributions and blinding in experiments

XW: Conceptualization; Data curation and analysis; Funding acquisition; Cell isolation; Experimental performances including measurements; Writing-original draft; Writing-review & editing. **JL:** Data curation and analysis; Cell isolation; Experimental performance including measurements; Writing review & editing. **QG:** Animal (WT and KO mice) care; Kidney collection; Project administration; Writing-review & editing. **HZ:** Data curation; Experimental performance including measurements; Writing-review & editing. **ZW:** Data curation and analysis; Experimental performance including measurements; Writing-review & editing. **MEG:** Conceptualization; Resources; Software; Visualization; Writing-review & editing. **CCYN:** Conceptualization; Project administration; Resources; Software; Supervision; Visualization; Writing-review & editing. **CD:** Conceptualization; Data curation and analysis; Funding acquisition; Project administration; Resources; Software; Supervision; Validation; Visualization; Writing original draft; Writing-review & editing.

References

1 Vizoso F.J. *et al*. Mesenchymal stem cells in homeostasis and systemic diseases: Hypothesis, evidences, and therapeutic opportunities. *Int. J. Mol. Sci.*20(15), 3738 (2019).

2 Murray P.A. & Woolf A.S. Using stem and progenitor cells to recapitulate kidney development and restore renal function. *Curr. Opin. Organ Transplant.*19(2), 140-144 (2014).

3 Brown C. *et al*. Mesenchymal stem cells: Cell therapy and regeneration potential. *J. Tissue Eng. Regen. Med.* 13(9), 1738-1755 (2019).

4 Dekel B. *et al*. Isolation and characterization of nontubular sca-1^{+}lin^{-} multipotent stem/progenitor cells from adult mouse kidney. *J. Am. Soc. Nephrol.* 17(12), 3300-3314 (2006).

5 Leuning D.G. *et al*. The human kidney capsule contains a functionally distinct mesenchymal stromal cell population. *PLOS one* 12(12), e187118 (2017).

6 Leuning D.G. *et al*. Clinical-grade isolated human kidney perivascular stromal cells as an organotypic cell source for kidney regenerative medicine. *Stem Cells Transl. Med*. 6(2), 405-418 (2017).

7 Huang Y. *et al*. Kidney-derived mesenchymal stromal cells modulate dendritic cell function to suppress alloimmune responses and delay allograft rejection. *Transplantation* 90(12), 1307-1311 (2010).

8 Huang Y. *et al*. Kidney-derived stromal cells modulate dendritic and T cell responses. *J. Am. Soc. Nephrol*. 20(4), 831-841 (2009).

9 Jiang M. H. *et al*. Nestin^{+} kidney resident mesenchymal stem cells for the treatment of acute kidney ischemia injury. *Biomaterials* 50, 56-66 (2015).

10 Wilson M.R. & Zoubeidi A. Clusterin as a therapeutic target. *Expert Opin. Ther. Targets* 21(2), 201-213 (2017).

11 Park S., Mathis K.W., & Lee I. K. The physiological roles of apolipoprotein J/clusterin in metabolic and cardiovascular diseases. *Rev. Endocr. Metab. Disord*. 15(1), 45-53 (2014).

12 Abdallah B.M., Alzahrani A.M. & Kassem M. Secreted Clusterin protein inhibits osteoblast differentiation of bone marrow mesenchymal stem cells by suppressing ERK1/2 signaling pathway. *Bone* 110, 221-229 (2018).

13 Jung G.S. *et al*. Clusterin attenuates the development of renal fibrosis. *J. Am. Soc. Nephrol*. 23(1), 73-85 (2012).

14 Guo J. *et al*. Relationship of clusterin with renal inflammation and fibrosis after the recovery phase of ischemia-reperfusion injury. *BMC Nephrol.* 17(1), 133 (2016).

15 Rosenberg M. E. *et al*. Apolipoprotein J/clusterin prevents a progressive glomerulopathy of aging. *Mol. Cell Biol.* 22(6), 1893-1902 (2002).

16 Nguan C.Y. *et al*. Promotion of cell proliferation by clusterin in the renal tissue repair phase after ischemia-reperfusion injury. *Am. J. Physiol. Renal Physiol*. 306(7), F724-F733 (2014).

17 Zhou W. *et al*. Loss of clusterin expression worsens renal ischemia-reperfusion injury. *Am. J. Physiol. Renal Physiol.* 298(3), F568-F578 (2010).

18 Gupta A. K. Fetal kidney stem cells ameliorate cisplatin induced acute renal failure and promote renal angiogenesis. *World J. Stem Cells* 7(4), 776 (2015).

19 Liu B. *et al*. Mesenchymal stroma cells in peritoneal dialysis effluents from patients. *Hum. Cell* 30(2), 51-59 (2017).

20 Liang P. *et al*. Prevention of Prostate Tumor Development by Stimulation of Antitumor Immunity Using a Standardized Herbal Extract (Deep Immune(R)) in TRAMP Mice. *Evid. Based Complement Alternat. Med.* 2018, 9707543 (2018).

21 Pittenger M. F. *et al*. Multilineage potential of adult human mesenchymal stem cells. *Science* 284(5411), 143-147 (1999).

22 Dominici M. *et al*. Minimal criteria for defining multipotent mesenchymal stromal cells. The International Society for Cellular Therapy position statement. *Cytotherapy* 8(4), 315-317 (2006).

23 Alnasser H. A. *et al*. Requirement of clusterin expression for prosurvival autophagy in hypoxic kidney tubular epithelial cells. *Am. J. Physiol. Renal Physiol*. 310(2), F160-F173 (2016).

24 Vizoso F. J. *et al*. Mesenchymal stem cell secretome: Toward cell-free therapeutic strategies in regenerative medicine. *Int. J. Mol. Sci.* 18(9), 1852 (2017).

25 Harrell C. R. *et al*. Molecular mechanisms responsible for therapeutic potential of mesenchymal stem cell-derived secretome. *Cells* 8(5), 467 (2019).

26 Huang J. *et al*. Stem/progenitor cell in kidney: characteristics, homing, coordination, and maintenance. *Stem Cell Res. Ther.* 12(1), 197 (2021).

27 Andrianova N. V. *et al*. Kidney cells regeneration: Dedifferentiation of tubular epithelium, resident stem cells and possible niches for renal progenitors. *Int. J. Mol. Sci.* 20(24), 6326 (2019).

28 Lee P. T. *et al*. Mouse kidney progenitor cells accelerate renal regeneration and prolong survival after ischemic injury. *Stem Cells* 28(3), 573-584 (2010).

29 Kitamura S. *et al*. Establishment and characterization of renal progenitor like cells from S3 segment of nephron in rat adult kidney. *FASEB J.* 19(13), 1789-1797 (2005).

30 Lazzeri E. *et al*. Endocycle-related tubular cell hypertrophy and progenitor proliferation recover renal function after acute kidney injury. *Nat. Commun.* 9(1), 1344 (2018).

31 Weng X. *et al*. Clusterin regulates macrophage expansion, polarization and phagocytic activity in response to inflammation in the kidneys. *Immunol. Cell Biol.* 99(3), 274-287 (2021).

32 Berebichez-Fridman R. & Montero-Olvera P. R. Sources and clinical applications of mesenchymal stem cells: State-of-the-art review. *Sultan Qaboos Univ. Med. J.* 18(3), e264-e277 (2018).

33 Mafi R. *et al*. Sources of adult mesenchymal stem cells applicable for musculoskeletal applications - a systematic review of the literature. *Open Orthop. J.* 5 Suppl 2, 242-248 (2011).

34 Plotkin M. D. & Goligorsky M. S. Mesenchymal cells from adult kidney support angiogenesis and differentiate into multiple interstitial cell types including erythropoietin-producing fibroblasts. *Am. J. Physiol. Renal Physiol.* 291(4), F902-F912 (2006).

35 Cakiroglu F. *et al*. Differences of cell surface marker expression between bone marrow- and kidney-derived murine mesenchymal stromal cells and fibroblasts. *Cell Mol. Biol.* 62(12), 11-17 (2016).

36 Bruno S., Chiabotto G. & Camussi G. Concise review: different mesenchymal stromal/stem cell populations reside in the adult kidney. *Stem Cells Transl. Med.* 3(12), 1451-1455 (2014).

37 Leong K. G. *et al*. Generation of a prostate from a single adult stem cell. *Nature* 456(7223), 804-808 (2008).

38 Pleniceanu O., Harari-Steinberg O. & Dekel B. Concise review: Kidney stem/progenitor cells: differentiate, sort out, or reprogram? *Stem Cells* 28(9), 1649-1660 (2010).

39 van de Rijn M. *et al*. Mouse hematopoietic stem-cell antigen Sca-1 is a member of the Ly-6 antigen family. *Proc. Natl. Acad. Sci. USA* 86(12), 4634-4638 (1989).

40 Putra A. *et al*. Hypoxia-preconditioned MSCs have superior effect in ameliorating renal function on acute renal failure animal model. *Open Access Maced J. Med. Sci.* 7(3), 305-310 (2019).

41 Aggarwal S. *et al*. Human $CD133^{+}$ renal progenitor cells induce erythropoietin production and limit fibrosis after acute tubular injury. *Sci. Rep.* 6, 37270 (2016).

42 Marcheque J. *et al*. Concise reviews: Stem cells and kidney regeneration: An update. *Stem Cells Transl. Med.* 8(1), 82-92 (2019).

43 Santeramo I. *et al*. Human kidney-derived cells ameliorate acute kidney injury without engrafting into renal tissue. *Stem Cells Transl. Med.* 6(5), 1373-1384 (2017).

44 Shrestha S. *et al*. Characterization and determination of cadmium resistance of $CD133^{+}/CD24^{+}$ and $CD133^{-}/CD24^{+}$ cells isolated from the immortalized human proximal tubule cell line, RPTEC/TERT1. *Toxicol. Appl. Pharmacol*. 375, 5-16 (2019).

45 Rodríguez-Rivera C. *et al*. Clusterin: Always protecting. Synthesis, function and potential issues. *Biomed Pharmacother.* 134, 111174 (2021).

46 Rohne P., Prochnow H. & Koch-Brandt C. The CLU-files: disentanglement of a mystery. *Biomol. Concepts* 7(1), 1-15 (2016).

47 Guan Q. *et al*. From humans to experimental models: The cytoprotective role of clusterin in the kidney. *Med. Surg. Urol.* 3(2), 134 (2014).

48 Li C. *et al*. Multiple roles of microRNA-100 in human cancer and its therapeutic potential. *Cell Physiol. Biochem.* 37(6), 2143-2159 (2015).

49 Fritz I. B. et al. Ram rete testis fluid contains a protein (clusterin) which influences cell-cell interactions *in vitro*. *Biol. Reprod.* 28(5), 1173-1188 (1983).

50 Dairi G. *et al*. Transcriptome-Based analysis of molecular pathways for clusterin functions in kidney cells. *J. Cell Physiol.* 231(12), 2628-2638 (2016).

51 Poulios E., Trougakos I. P. & Gonos E. S. Comparative effects of hypoxia on normal and immortalized human diploid fibroblasts. *Anticancer Res.* 26(3A), 2165-2168 (2006).

52 Mohyeldin A., Garzon-Muvdi T. & Quinones-Hinojosa A. Oxygen in stem cell biology: A critical component of the stem cell niche. *Cell Stem Cell* 7(2), 150-161 (2010).

53 Ezashi T., Das P. & Roberts R. M. Low O_2 tensions and the prevention of differentiation of hES cells. *Proc. Natl. Acad. Sci. USA* 102(13), 4783-4788 (2005).

54 Zhang W. & Edwards A. Oxygen transport across vasa recta in the renal medulla. *Am. J. Physiol. Heart Circ. Physiol.* 283(3), H1042-H1055 (2002).

55 Geng Y. *et al*. Mesenchymal stem cells ameliorate rhabdomyolysis-induced acute kidney injury via the activation of M2 macrophages. *Stem Cell Res.* Ther. 5(3), 80 (2014).

56 Sica A. & Mantovani A. Macrophage plasticity and polarization: *in vivo veritas*. *J. Clin. Invest.* 122(3), 787-795 (2012).

57 Ferrante C. J. & Leibovich S. J. Regulation of macrophage polarization and wound healing. *Adv. Wound Care (New Rochelle)* 1(1), 10-16 (2012).

Tables

Table 1: A panel of MSC marker expression of renal MSC after P4 in WT and KO.

Antibodies	WT	KO
CD133	88.7 ± 7.2	77.9 ± 4.5
Sca-1	95.2 ± 8.5	72.0 ± 6.7
CD44	98.2 ± 10.3	87.2 ± 7.6
CD117	53.0 ± 5.2	64.1 ± 6.4
CD34	7.43 ± 2.4	5.02 ± 3.4
CD45	1.61 ± 0.4	1.07 ± 0.9
CD163	1.87 ± 0.2	2.49 ± 1.2
CD41	2.39 ± 0.6	1.18 ± 0.8
CD276	4.25 ± 1.3	1.11 ± 0.8
CD138	2.75 ± 0.4	0.39 ± 1.2
CD79a	1.36 ± 0.8	1.24 ± 0.7

Data were presented by mean ± SD (%) (n = 3). No statistical difference between WT and KO cells was seen in the positive expression of CD133, Sca-1, CD44 and CD117.

Figures

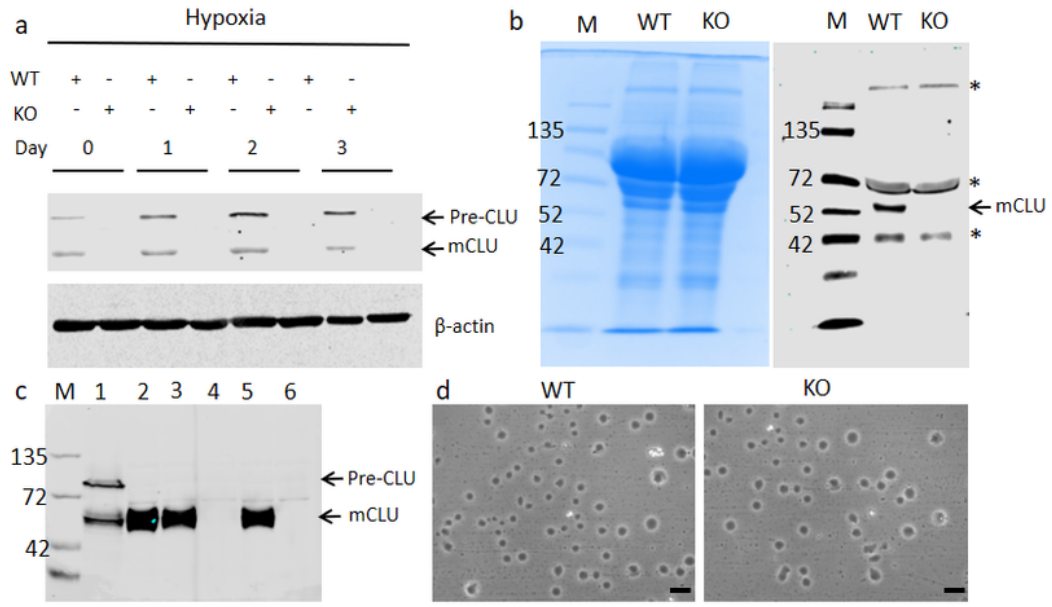

Full-length blots for Figure 1a

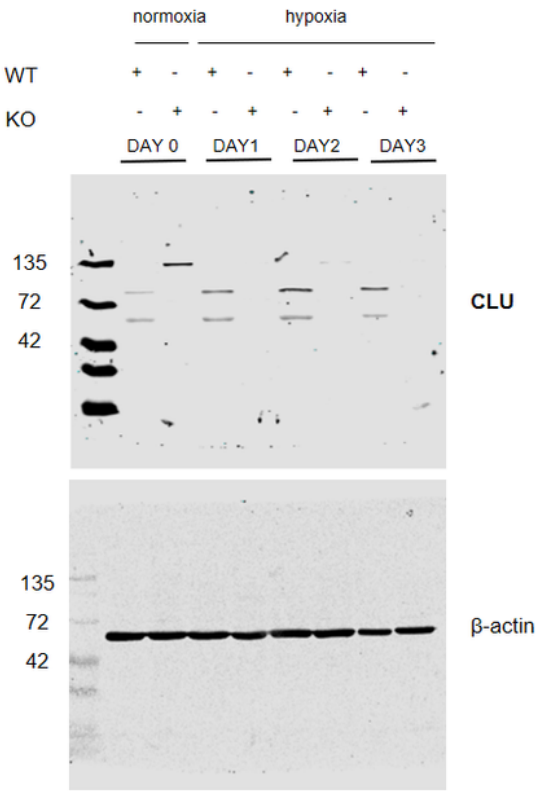

Cropped blots for Figure 1a

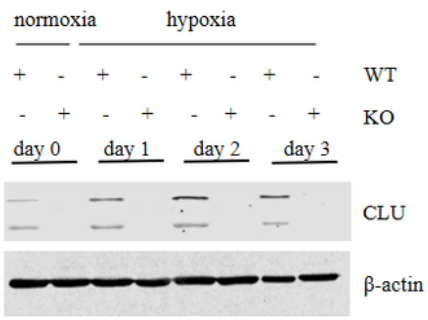

Figure 1

The expression of intracellular and secreted CLU protein in cultured WT KMSCs and KO KMSCs. (a) Both WT KMSCs and KO KMSCs were exposure to hypoxia (1% oxygen) from 0 (normoxia) to 1, 2 and 3 days, followed by extraction of total cellular protein. The CLU proteins in the cellular protein extracts were detected by Western blot with anti-CLU (sc-6419) antibody, and β-actin was reprobed in the same membrane. (b) Secreted mCLU in culture supernatants, which was precipitated by 80% saturated

ammonium sulfate solution, was detected by Western blot. Left image: Coomassie brilliant blue-stained proteins, right image: CLU protein. (c) CLU proteins in protein extracts of cultured WT KMSCs (lane 1), dead cells/cell debris pellets (lane 2), culture supernatant after pelleting the dead cells/cell debris (lane 3), microvesicle pellet (lane 4), culture supernatant after pelleting the microvesicles (lane 5), and culture medium containing 5% pooled serum of CLU KO mice (lane 6). (d) Typical microscopic views of microvesicles from conditional medium of both WT and KO KMSCs. WT: WT KMSCs, KO: KO KMSCs, Pre-CLU: CLU precursor, mCLU: mature CLU, *: non-specific proteins or CLU from FBS. M: protein size marker (kDa). Bar: 500 nm. Data are representative of three independent experiments (one mouse per each experiment, n = 3 mice).

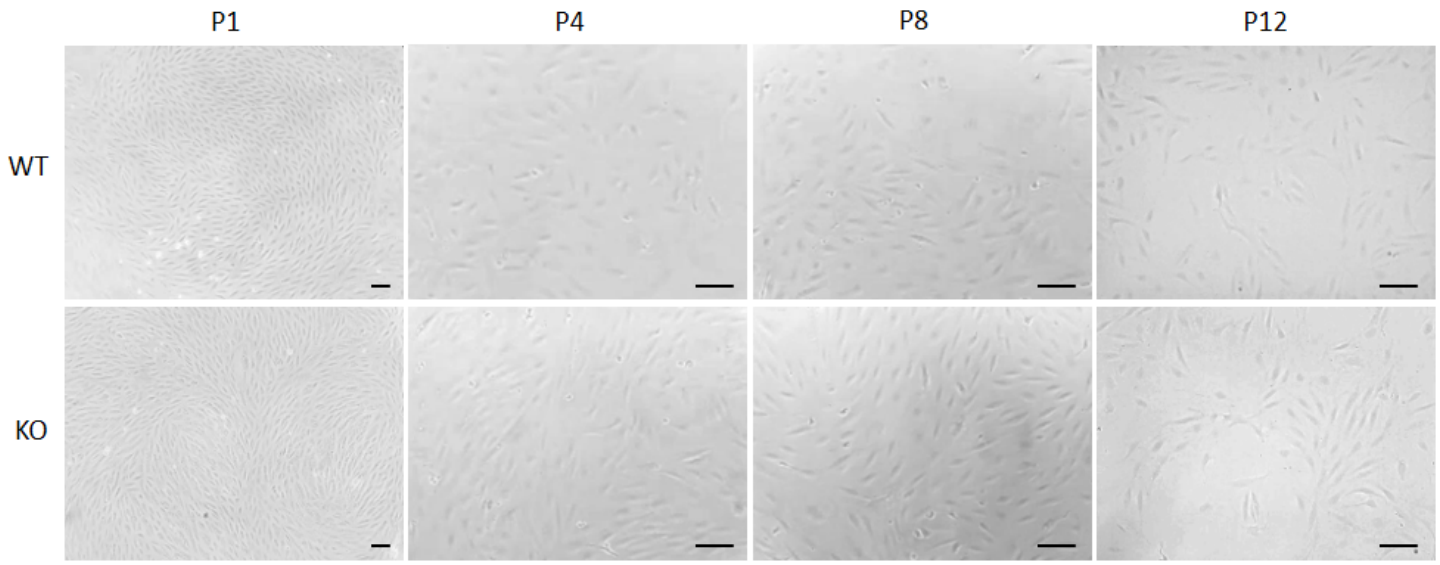

Figure 2

A typical microscopic view of KMSCs morphology from cultures in different passage. The typical morphology of WT KMSCs (WT, upper panel), and KO KMSCs (KO, bottom panel). P: culture passage. Scale bar: 20 μm. Data are representative of four independent experiments (one mouse per each experiment, n = 4 mice).

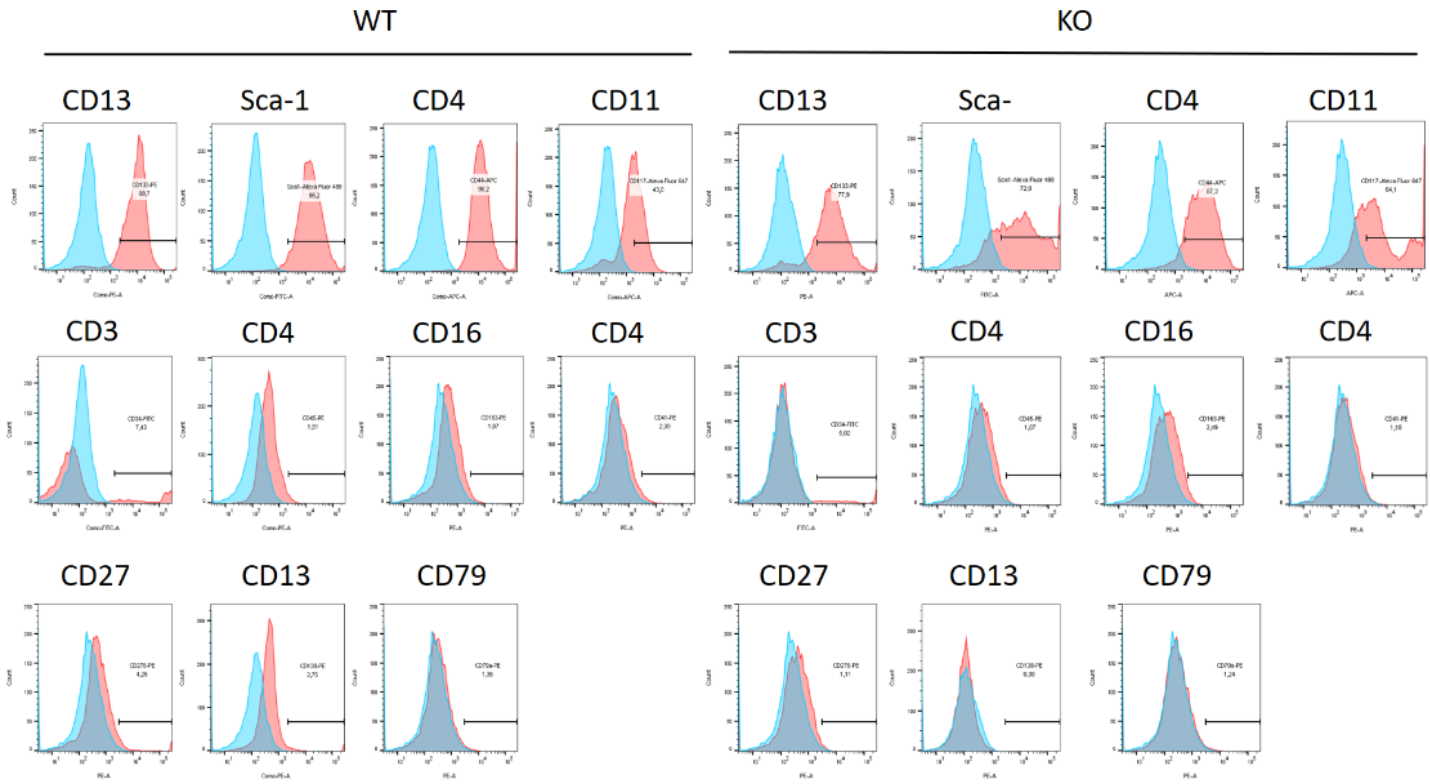

Figure 3

Typical histograms of MSC surface marker expression in KMSC from WT (n = 3) and KO mice (n = 3). The expression of a panel of MSC markers in unsorted WT and KO KMSCs was investigated after P4. Blue: background staining.

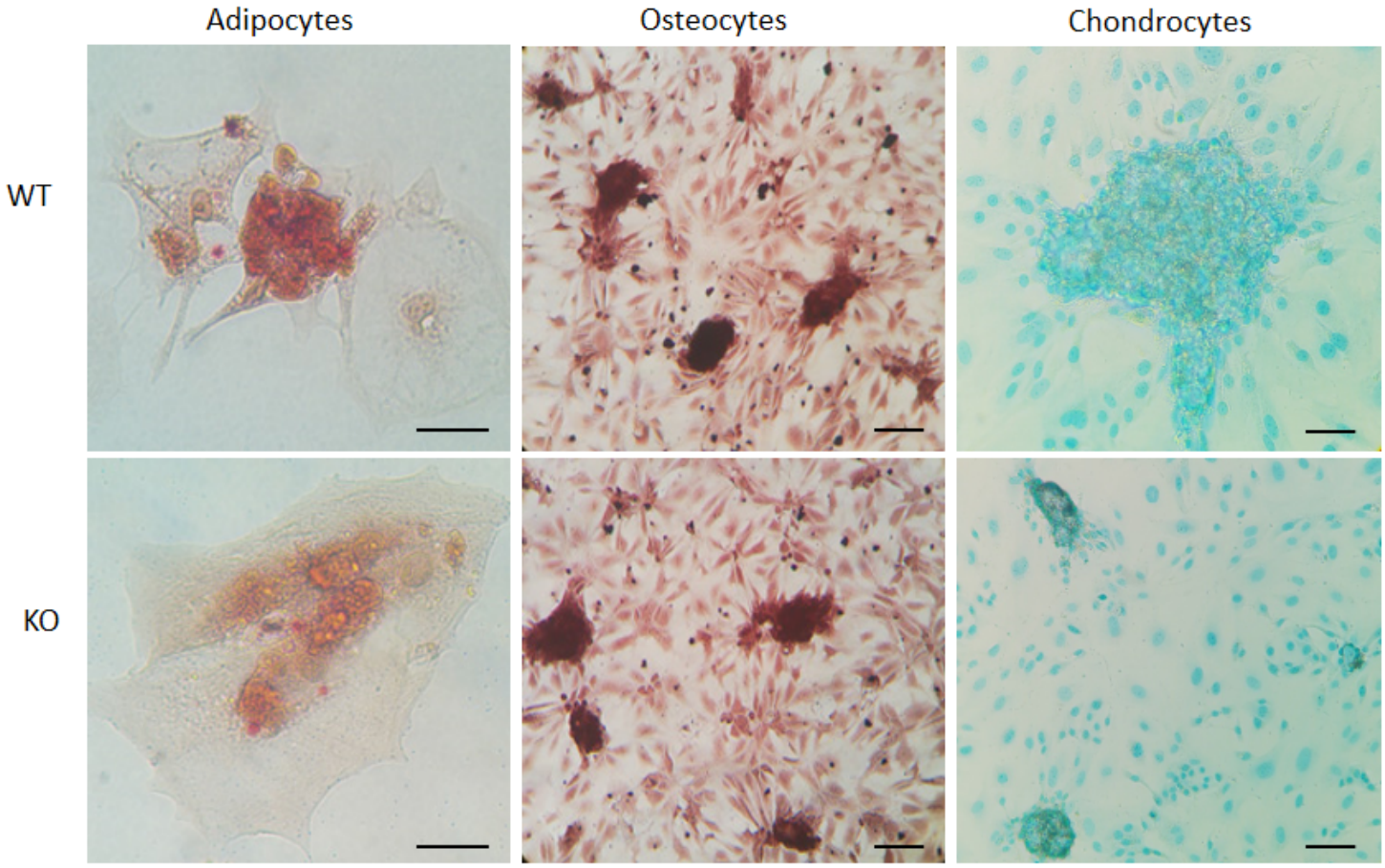

Figure 4

A typical microscopic view of differentiated cell staining. KMSCs from P4 were induced to chondrocytes, adipocytes, or osteocytes by incubation with each different differentiation medium for four weeks. Differentiation to adipocytes from both WT and KO KMSCs were confirmed by positive stain with Oil red O, to osteocytes by positive stain with Alizarin red S. Red, and to chondrocytes by positive stain with Alcian blue. Scale bar: 20 μm. Data are representative of four independent experiments (one mouse per each experiment, n = 4 mice)

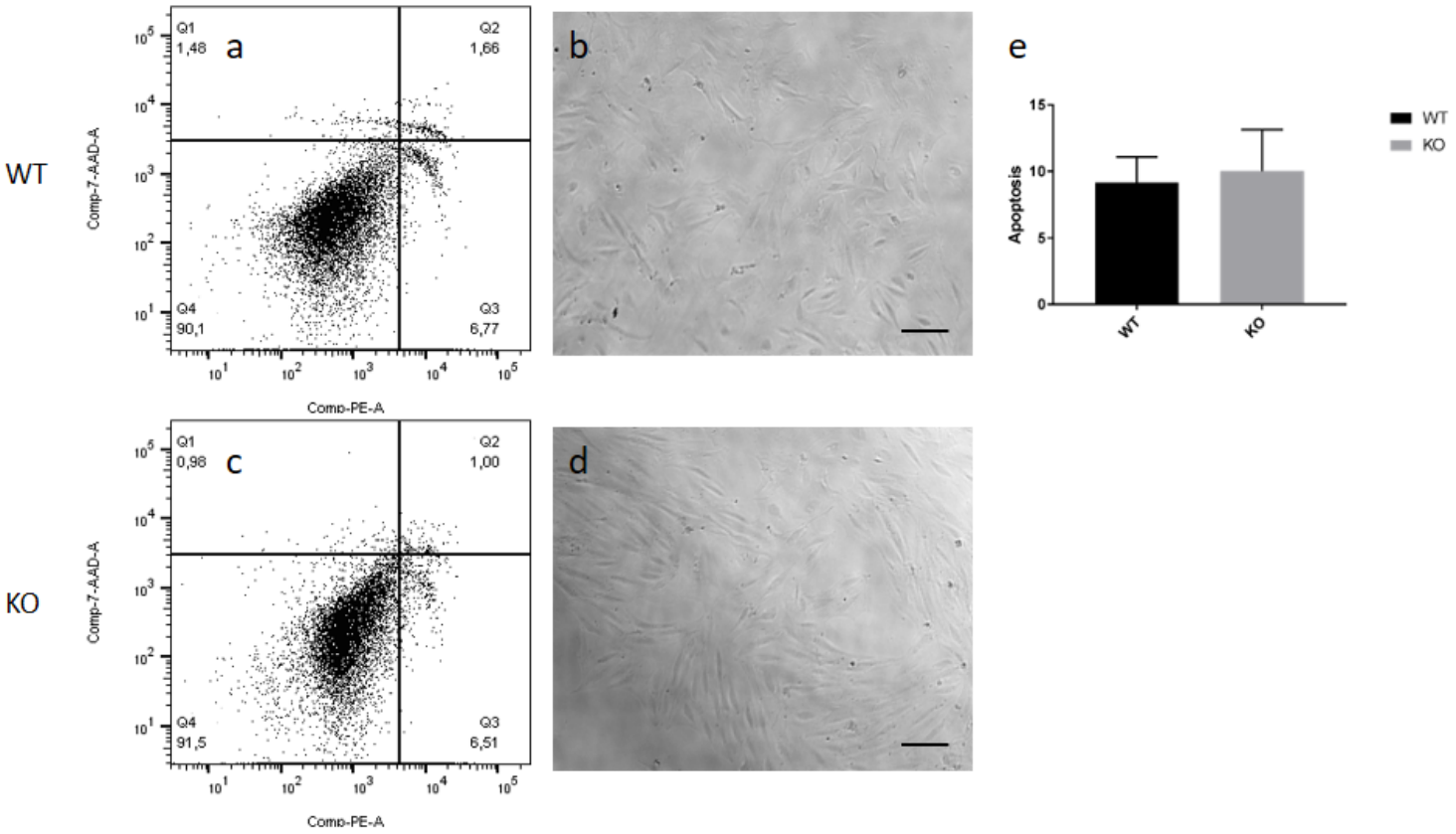

Figure 5

Cell survival in WT and KO KMSCs in hypoxia. (a, c) FACS analysis of cell viability and death of KMSCs from WT (a) and KO (c) groups after 3-day exposure to hypoxia. (b, d) The light microscopic views of the KMSCs of WT (b) and KO (d) group after incubation with hypoxia for three days. Data in a, b, c and d are representative of three independent experiments (one mouse per each experiment, n = 3 mice). Scale bar: 20 μm. (e) Statistical comparison of cell apoptosis, as indicated by total annexin-V positive staining, in all three separate examinations. Data are presented as means ± SD (standard deviation) in each group. P = 0.5257 (WT vs. KO, two-tailed t-test, n = 3).

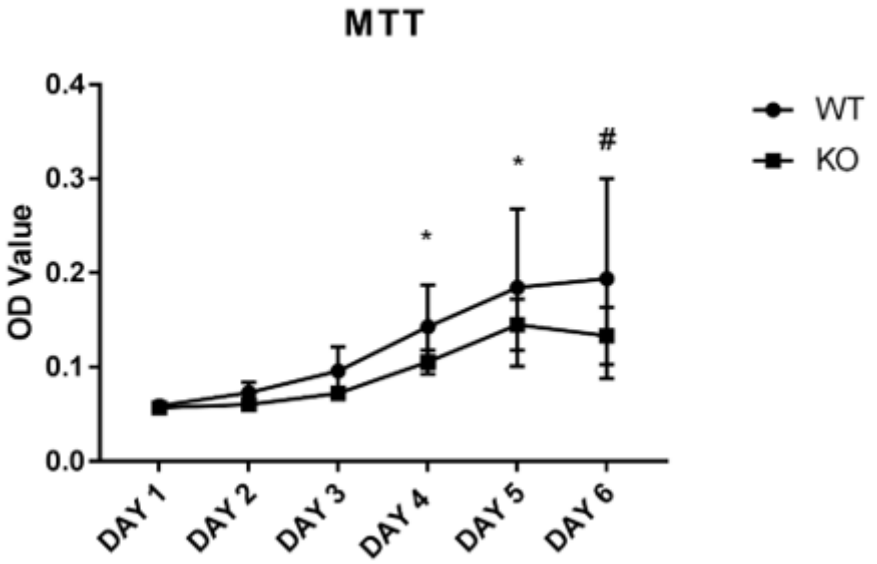

Figure 6

The proliferation was measured by using the MTT assay. KMSCs were isolated from 3 mice in each group. In each experiment using the KMSCs from each individual mouse, the OD 490 value was measured, and the data were presented as mean ± standard error of the mean (SEM) of three separate experiments in each group (WT vs. KO: P = 0.0174, Two-way ANOVA, n = 3 mice). *P < 0.05 (WT vs. KO, two-tailed t-test, n = 3 mice), #P < 0.01 (WT vs. KO, two-tailed t-test, n = 3 mice).

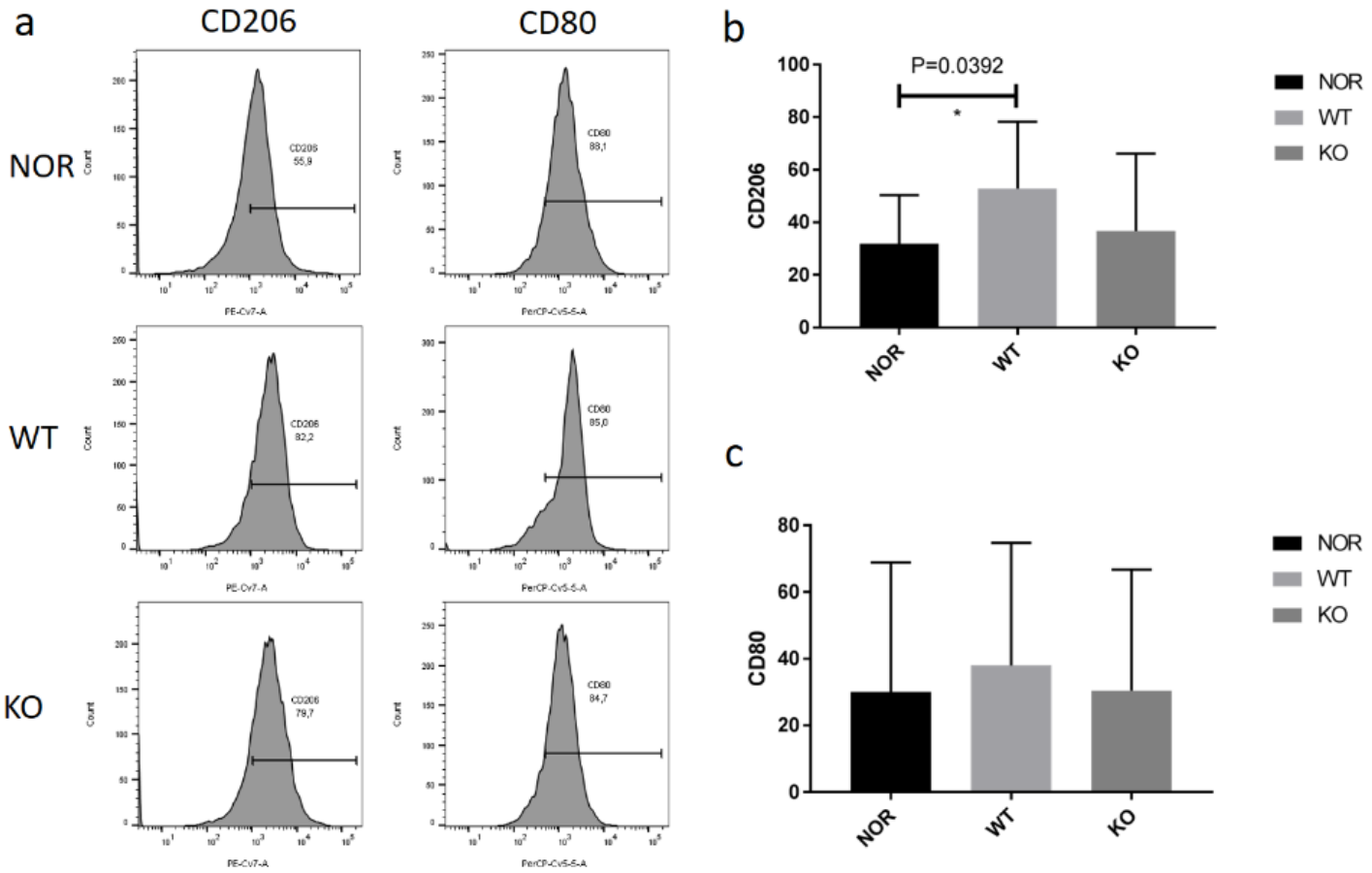

Figure 7

The phenotype change of macrophage affected by the conditional medium from KMSCs of WT and KO was examined by using FACS. (a) A typical histogram of CD206 and CD80 of each group. Data are representative of three independent experiments (one mouse per experiment, n = 3 mice). (b, c) The data of CD206 and CD80 are presented as mean ± SEM of three separate experiments in each group. *P = 0.0392 (NOR vs. WT, two-tailed t-test, n = 3).

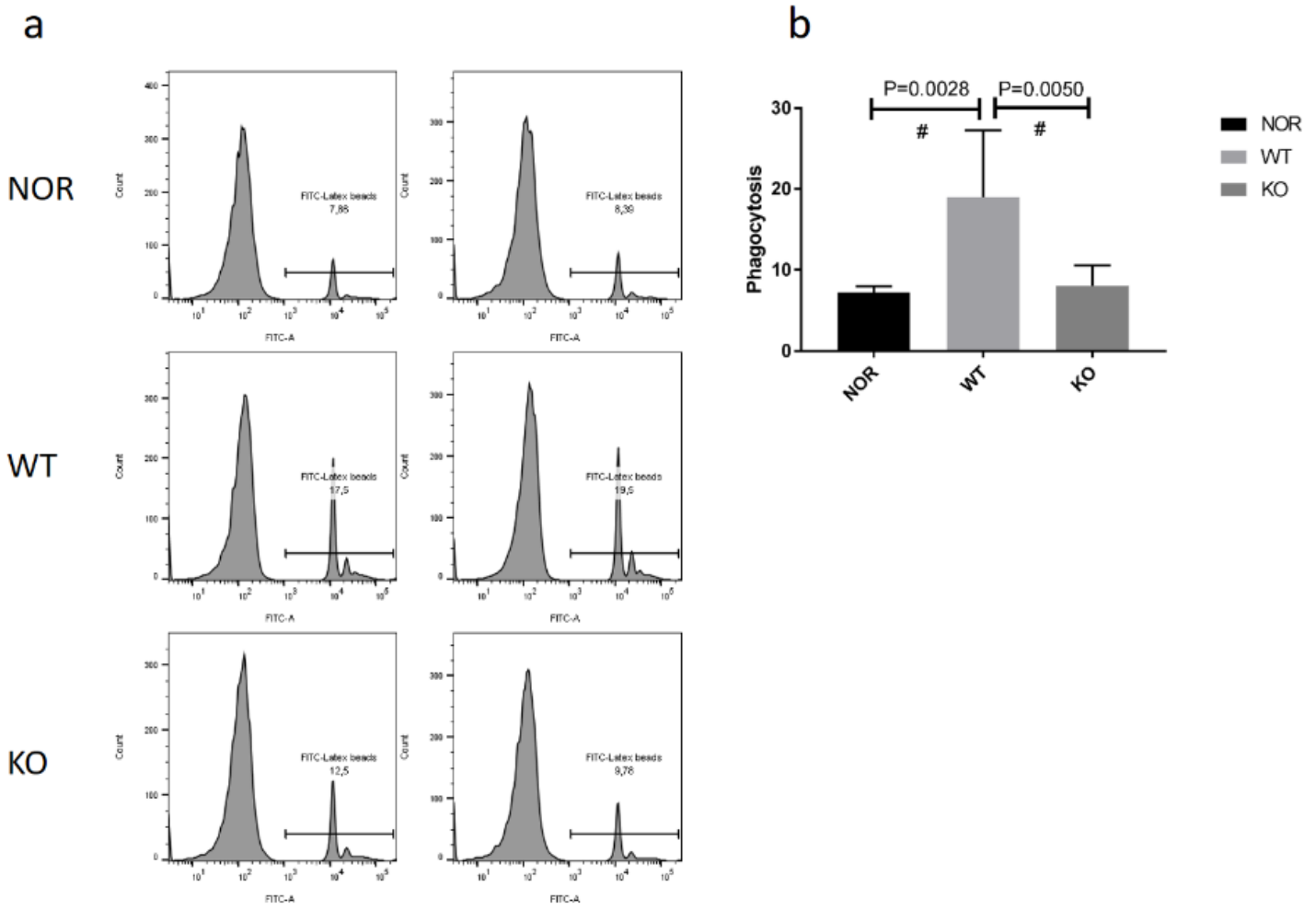

Figure 8

The phagocytosis of macrophage which affected by the conditional medium from KMSCs of WT and KO mice, was examined by using FACS. (a) A typical histogram of phagocytosis of each group. Data are representative of three independent experiments (one mouse per experiment, n = 3 mice). (b) The data of phagocytosis are presented as mean ± SEM of three independent experiments in each group. #P = 0.0028 (NOR vs. WT, two-tailed t-test, n = 3); #P = 0.0050 (WT vs. KO, two-tailed t-test, n = 3).

Supplementary Files

This is a list of supplementary files associated with this preprint. Click to download.

- SupplementarydataFig1.pptx